Transient dynamics and nonlinear stability of spatially extended systems

Andreas Handel

Department of Biology, Emory University, Atlanta, Georgia 30322, USA

Roman O. Grigoriev

School of Physics, Georgia Institute of Technology, Atlanta, Georgia 30332-0430, USA

(Received 9 May 2006; published 14 September 2006)

As studies of various systems have shown, the sole focus on the eigenvalues in a linear stability analysis can be misleading, especially when the dynamics of disturbances is characterized by strong transient growth. The aim of this paper is to extend the generalized stability analysis, in the context of spatially extended systems, by examining the role of the nonlinear terms in the destabilization process. The critical noise level leading to destabilization is often found to scale as a power of the magnitude of transient amplification. In what follows we show that the power law exponent sensitively depends on the type of nonlinear terms and their potential for generating self-sustaining noise amplification cycles (bootstrapping). We find, however, that the exponents are not universal and also depend on the more subtle details of the transient dynamics. We also show that the basin of attraction of a spatially uniform state is bounded by the stable manifold(s) of nearby saddle(s) which play a major role in the transition.

I. INTRODUCTION

The problem of nonlinear stability of spatially extended systems characterized by strong transient amplification of disturbances has attracted a lot of attention recently, primarily in the context of transition to turbulence in shear flows [1–3]. Such transitions provide a vivid example of the failure of linear stability analysis. While there is more or less universal agreement that many experimental situations involve the "bypass" transition scenarios not based on a linear instability of the laminar flow profile, the details of these scenarios are still debated. One possible explanation involves an essentially linear transition mechanism based on transient growth of spontaneous disturbances [4]. Another explanation suggests that the transition is primarily due to the nonlinearity of the evolution equations which introduces nearby states which are linearly unstable [5].

Despite significant progress in understanding transient growth caused by the strongly non-normal linear part of the evolution equations [6,7], the role of the nonlinear terms is still poorly understood. The progress in understanding the details of the bypass transition mechanism(s) in the case of shear flows has been limited both due the complexity of the Navier-Stokes equation and the difficulty of characterizing the dynamics of small disturbances in experimental flows [8,9]. It would seem fair to say that currently there does not exist a description of transition capable of producing quantitative predictions for either the spatial structure or the magnitude of critical disturbances in shear flow. Most previous attempts at a quantitative description were based on low-dimensional phenomenological models [10] instead of a systematic analysis of the dynamics of a spatially extended system. The few studies (e.g., Ref. [11]) that do analyze the full Navier-Stokes equations are not capable of predicting quantitatively the critical size of disturbances leading to transition either, only the scaling with the Reynolds number.

The aim of this paper is to describe quantitatively and rigorously the combined effect of transient growth and nonlinearity in a model spatially extended system, described by a partial differential equation, by taking into account both the temporal and spatial aspects of the dynamics. To obtain such an analytically tractable model, we will consider a problem of boundary feedback control of a spatially extended system introduced in Refs. [12,13], which is also characterized by strong transient growth of disturbances.

The paper is organized as follows. Section II introduces the model and summarizes the results of its numerical analysis. Section III describes transient dynamics displayed by the model in the linear approximation. The nonlinear stability analysis for the case of a cubic nonlinearity is presented in Sec. IV. The stability analysis is repeated in Sec. V for the case of quadratic nonlinearity. Finally, our conclusions are presented and their connection to the shear flow problems is discussed in Sec. VI.

II. THE MODEL

Consider a generalized form of the Ginzburg-Landau equation

$$\partial_t \phi = \phi + \partial_x^2 \phi + f(\phi), \tag{1}$$

where $f(\phi)$ denotes the nonlinear terms [the standard version has $f(\phi) = -\phi^3$]. As we have shown in a series of earlier papers [12–14], the uniform state $\phi = 0$ of Eq. (1) can be made linearly stable by imposing feedback control at one, or both, boundaries. For instance, one could choose the boundary conditions in the form

$$\phi(0,t) = 0, \quad \phi'(L,t) = \int_0^L k(x)\phi(x,t)dx, \tag{2}$$

where $k(x)$ is an appropriately chosen gain function. The eigenmodes and eigenvalues of the linearized system are given, respectively, by $\psi_n(x) = \sin(q_n x)$ and $\lambda_n = 1 - q_n^2$, $n = 1, 2, \ldots$. Without feedback, $k(x) = 0$, the wave numbers

are given by $q_n = (n - \frac{1}{2}) \pi / L$, while applying feedback allows one to chose them completely arbitrarily, subject to the condition $\lambda'_n = 1 - q'^2_n$, $n = 1, 2, \ldots$ (we will use the prime to denote the eigenmodes, eigenvalues, and wave numbers of the closed loop system).

The closed loop eigenmodes are not orthogonal as long as $q_n \neq q'_n$ for at least one n, indicating that the evolution operator of the closed loop system is non-normal and as a consequence generic disturbances undergo transient growth even when all closed loop eigenvalues are negative. The easiest way to control the degree of non-normality, and through it the magnitude of transient amplification

$$\gamma_p(t) \equiv \max_{\phi(x,0)} \frac{\|\phi(x,t)\|_p}{\|\phi(x,0)\|_p}, \qquad (3)$$

is by tuning the length of the system L. (Different choices of the norm $\|\cdot\|_p$ can be useful for characterizing different aspects of transient dynamics.) Larger values of L result in a larger number of unstable modes whose wave numbers need to be shifted into the stable band $q > 1$, thereby increasing the degree of non-normality. As a consequence, the maximum transient amplification

$$\Gamma_p = \max_t \gamma_p(t) \qquad (4)$$

also increases (for instance, Γ_2 grows exponentially with the system size L, as we have shown elsewhere [12,14]).

Another important finding was that for large L the critical noise level $\sigma_2 \equiv \|\phi(x,0)\|_2$ resulting in a loss of control (i.e., destabilization of the uniform state $\phi = 0$ followed by transition to a nonuniform state) follows a power law dependence $\sigma_2 \sim \Gamma_2^\kappa$ with an exponent κ depending on the type of nonlinearity. According to the simple arguments presented in the original study [13], the exponent for a quadratic nonlinearity should have a value of $\kappa = -2$, consistent with the bootstrapping scenario [2] in which the nonlinear term is treated as a source of secondary disturbances which can undergo further transient amplification. The cubic nonlinearity (as well as any other odd power nonlinearity), on the other hand, was found to yield the smallest value of the exponent, $\kappa = -1$, suggesting a purely linear mechanism of instability. In this paper we try to better understand the origins of the scaling behavior and investigate whether the scaling exponents are universal (i.e., depend only on the power of the nonlinearity).

III. TRANSIENT DYNAMICS IN THE LINEAR APPROXIMATION

Our goal in this section is to characterize the transient behavior of our spatially extended system in the linear approximation using the parameters describing the non-normality of the evolution operator. To construct an analytically tractable description of the system described by Eqs. (1) and (2) we choose the length of the system L to be such that there is only one unstable eigenmode ψ_1, while the mode ψ_2 is weakly stable. This can be achieved by taking $q_2 = 1 + \alpha$, with α small and positive, which corresponds to

choosing $L = \frac{3}{2} \pi / (1 + \alpha)$. Next we choose the feedback gain in such a way that the wave number of the unstable mode is moved into the stable band, $q'_1 = 1 + \alpha + \epsilon$ with some positive ϵ, while the rest of the modes are unaffected, $q'_n = q_n$, $n = 2, 3, \ldots$. With these choices the two parameters $\alpha = 1 - q'^2_2$ and $\epsilon = q'_1 - q'_2$ characterize, respectively, the stability properties and the non-normality of the Jacobian of the linearized system, which can be tuned independently.

To avoid confusion about the relative magnitude of the two small parameters α and ϵ in the perturbative calculations we will assume that their ratio $\beta = \epsilon / \alpha$ is $O(1)$ relative to the magnitude of α and use α as the small parameter. As we will see below, despite this assumption the analytical results will be accurate for β ranging by many orders of magnitude.

With the feedback turned on and for α and ϵ small, the strongly damped modes $\psi'_3, \psi'_4, \ldots$ are slaved to the dynamics of the weakly damped modes ψ'_1 and ψ'_2, and can be adiabatically eliminated (conceptually similar approaches have been pursued in the context of shear flows as well [15,16]). We demonstrate this process by keeping only one fast mode ψ'_3. The corresponding three-mode truncation has been verified numerically to provide an accurate representation of the dynamics of the spatially extended system, obviating the need for more cumbersome models based on higher-order truncations.

In order to determine the evolution equations for the modes ψ'_1, ψ'_2, and ψ'_3, we start by substituting the truncated expansion

$$\phi(x,t) = \sum_{n=1}^{3} a_n(t) \psi'_n(x) \qquad (5)$$

into Eq. (1). Multiplying by $\psi_m(x)$ and integrating from 0 to L one obtains a system of nonlinear ordinary differential equations for the amplitudes a_1, a_2, and a_3:

$$A\dot{\mathbf{a}} = A\Lambda' \mathbf{a} + \mathbf{F}(\mathbf{a}), \qquad (6)$$

where $\mathbf{a} = (a_1, a_2, a_3)^T$

$$A = \begin{pmatrix} -\dfrac{9}{4}\beta\alpha & 0 & 0 \\[2mm] 1 + \dfrac{1}{2}\beta\alpha & 1 & 0 \\[2mm] \dfrac{9}{8}\beta\alpha & 0 & 1 \end{pmatrix}, \quad \Lambda' = \begin{pmatrix} \lambda'_1 & 0 & 0 \\ 0 & \lambda'_2 & 0 \\ 0 & 0 & \lambda'_3 \end{pmatrix}, \quad (7)$$

$\lambda'_1 = -2(\beta + 1)\alpha$, $\lambda'_2 = -2\alpha$, $\lambda'_3 = -16/9$, and $\mathbf{F}(\mathbf{a})$ represents the nonlinear terms. Here and in the subsequent calculations we will only present results to leading order in α.

Although the linearization $\dot{\mathbf{a}} = \Lambda' \mathbf{a}$ of Eq. (6) is normal (and hence the norm of $\mathbf{a}$ decays monotonically when Λ' is stable), the corresponding dynamics of the physically relevant quantity $\|\phi(x,t)\|_2$ in the original space spanned by the eigenmodes $\{\psi_n\}$ displays transient behavior, typically showing fast initial growth in the amplitude of disturbances followed by slow exponential decay. The differences in the dy-

namics of $\|a\|_p$ and $\|\phi\|_p$ are due to the nonnormality of the transformation matrix [17,18]. In our three mode truncation one obtains simply $\gamma_p(t) = \|U(t)\|_p$, where

$$U(t) = Ae^{\Lambda' t}A^{-1}, \tag{8}$$

is the matrix representation of the finite time evolution operator in the basis of the open loop system. The matrix U has five nonzero elements, three on the diagonal $U_{nn} = e^{\lambda'_n t}$, $n = 1, 2, 3$, and two more in the first column

$$U_{21} = \frac{4}{9\beta\alpha}(e^{\lambda'_2 t} - e^{\lambda'_1 t}), \tag{9}$$

$$U_{31} = \frac{1}{2}(e^{\lambda'_3 t} - e^{\lambda'_1 t}).$$

For $\alpha \ll 1$ the term U_{21} dominates, so regardless of the norm used in this limit one obtains

$$\gamma_p(t) \approx |U_{21}| = \frac{4}{9\beta\alpha}|e^{-2\alpha t} - e^{-2(\beta+1)\alpha t}|. \tag{10}$$

The maximum

$$\Gamma_p = \Gamma = \frac{4}{9\alpha}(1 + \beta)^{-(1+\beta^{-1})} \tag{11}$$

is achieved at

$$t_{\max} = \frac{1}{2\alpha}\frac{\ln(1 + \beta)}{\beta}. \tag{12}$$

For comparison purposes we compute the transient amplification Γ_2 numerically using the PDE (1). (The two-norm will be used exclusively in the remainder of this paper as it greatly simplifies both analytical and numerical calculations.) The results are shown in Fig. 1. As one can see, the three mode truncation faithfully reproduces the transient amplification observed in the original model.

As Eq. (11) shows, transient amplification can become arbitrarily large for small enough ϵ and α. The time $t_{\max}$ also diverges in this limit. Both achieve their largest values $\Gamma = 4/(9e\alpha)$ and $t_{\max} = 1/(2\alpha)$ for $\beta \to 0$, which corresponds to $\epsilon \ll \alpha$. On the other hand, for $\epsilon \gg \alpha$ one obtains $\Gamma = 4/(9\epsilon)$ and, up to logarithmic corrections in α, $t_{\max} = 1/(2\epsilon)$.

The optimal disturbance characterized by the largest transient amplification is given by the right singular vector of $U(t_{\max})$ corresponding to the largest singular value, in our case $(1, 0, 0)^T$. Not surprisingly, this optimal disturbance corresponds to the unstable eigenmode ψ_1 of the open loop system. The evolution amplifies this initial optimal disturbance by a factor of Γ and rotates it in the direction defined by the respective left singular vector $(0, 1, 0)^T$ which corresponds to the weakly damped eigenmode ψ_2.

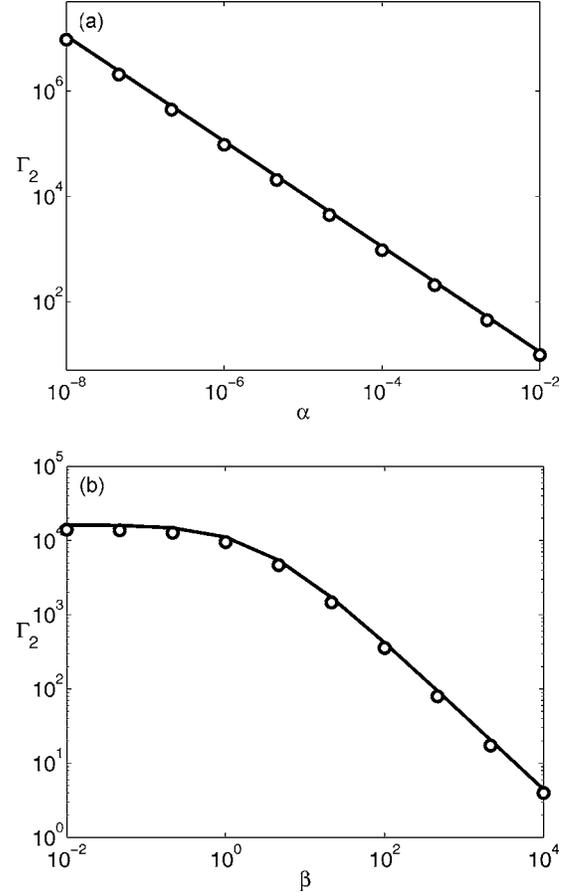Converting into the basis of eigenmodes $\{\psi'_n\}$ of the closed loop system, we obtain the optimal disturbance

FIG. 1. Transient amplification factor Γ_2 (a) as a function of α with $\beta = 1$. (b) Same as a function of β for $\alpha = 10^{-5}$. The circles show the maximal transient amplification achieved in the linearized version of the PDE (1) and the solid curve represents the analytical result (11).

$$\mathbf{a}_{\text{in}} = A^{-1}\begin{pmatrix} 1 \\ 0 \\ 0 \end{pmatrix} = \frac{4}{9\epsilon}\begin{pmatrix} -1 \\ 1 \\ 0 \end{pmatrix} + O(1), \tag{13}$$

which lies near the surface $a_1 + a_2 = 0$. At $t = t_{\max}$ this initial disturbance is transformed (in the absence of nonlinear terms) into

$$\mathbf{a}_{\text{out}} = A^{-1}\begin{pmatrix} 0 \\ 1 \\ 0 \end{pmatrix} = \begin{pmatrix} 0 \\ 1 \\ 0 \end{pmatrix}. \tag{14}$$

This result might look confusing at first glance: the initial disturbance $\mathbf{a}_{\text{in}}$ appears larger than the "amplified" disturbance $\mathbf{a}_{\text{out}}$. In fact the opposite is true, since the norm is computed in a different space.

IV. TRANSIENT DYNAMICS WITH A CUBIC NONLINEARITY

Having understood the dynamics of the linearization, we can now turn to the analysis of the effects of nonlinearity. Here we are going to investigate the cubic and the quadratic

nonlinearity which, for $L \gg 1$, represent the two extremes of scaling behavior in our model [13]. It is of particular interest to determine whether the scaling exponents persist for systems of size $L = O(1)$.

We begin by rewriting Eq. (6) for the cubic nonlinearity, which to leading order in α gives

$$\dot{a}_1 = \lambda_1' a_1 - \frac{1}{3\epsilon} s^2 a_3 + \frac{39}{40} s^2 a_1,$$

$$\dot{a}_2 = \lambda_2' a_2 + \frac{1}{3\epsilon} s^2 a_3 - \frac{39}{40} s^2 a_1 + \frac{3}{4} s^3,$$

$$\dot{a}_3 = \lambda_3' a_3 + \frac{15}{8} s^2 a_3 + \frac{3}{4} a_3^3 - \frac{2187}{2240} \epsilon s^2 a_1, \quad (15)$$

where we have defined $s \equiv a_1 + a_2$. Since λ_3' is much larger (in absolute value) than both λ_1' and λ_2', the mode ψ_3' can be adiabatically eliminated by assuming a_1 and a_2 to be constant. We then find that the third equation in Eq. (15) has three fixed points, a stable one at

$$a_3 = \frac{19683 \epsilon s^2 a_1}{280(135 s^2 - 128)} \quad (16)$$

and two unstable ones at

$$a_3 = \pm \frac{1}{18} \sqrt{768 - 810 s^2}, \quad (17)$$

for $|s| < s^* \equiv 8\sqrt{30}/45 \approx 0.97$. As $|s|$ increases past the critical value s^*, the outside fixed points (17) merge and disappear in a pitchfork bifurcation, while the middle fixed point (16) becomes unstable.

The solution of the truncated model (15) can converge to the origin only if the trajectory stays at all times inside the band $|a_1 + a_2| < s^*$ in the (a_1, a_2) plane. If the trajectory leaves this band, a_3 immediately blows up, causing a_1 and a_2 to blow up as well and leading to a quick divergence away from the uniform state $\phi = 0$.

While this is one possible mechanism of instability, it turns out that in this particular example the dominant instability mechanism is different. As long as the trajectory lies inside the band, we can substitute the stable fixed point value (16) for a_3 into the first two equations in Eq. (15). Aside from a stable node at the origin, $a_1 = a_2 = 0$, these equations have a pair of saddle fixed points at

$$a_1^s = 0, \quad a_2^s = \pm \frac{2}{3} \sqrt{6} \sqrt{\alpha} \quad (18)$$

and a pair of unstable nodes at

$$a_1^n = \pm \frac{4(10\beta - 3)}{507\beta} \sqrt{195(\beta + 1)} \sqrt{\alpha},$$

$$a_2^n = \pm \frac{12(\beta + 1)}{507\beta} \sqrt{195(\beta + 1)} \sqrt{\alpha}. \quad (19)$$

As Fig. 2 shows, the stable manifolds of the saddles (18) originate at the nodes (19) and serve as the boundaries of the
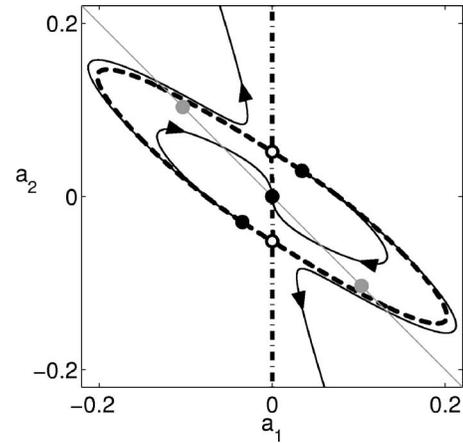

FIG. 2. The phase portrait of the system with the cubic nonlinearity for $\alpha = 10^{-3}$ and $\beta = 1$. Closed and open black circles denote the nodes and saddles, respectively, of the truncation (15). The dashed and dash-dotted lines show, respectively, the stable and unstable manifolds of the saddles. The solid black curves show a few sample trajectories of the PDE (1). Finally, the gray circles represent the estimate (22) of the intersection between the stable manifold and the antidiagonal $a_1 = -a_2$ (solid gray line).

basin of attraction for the stable node at the origin. The critical disturbance in this case corresponds to a trajectory that evolves along a separatrix defined by the stable manifold of one of the saddle fixed points. In particular, the minimum of the norm

$$\sigma_2 = \min_t \|\phi(t)\|_2 = \min_t \sqrt{\frac{L}{2}} \|A\mathbf{a}(t)\|_2 \quad (20)$$

over the stable manifold determines the magnitude of the optimal initial perturbation in the presence of the cubic nonlinearity.

The analytical computation of the stable manifold is too complicated to be of any use here. Instead we use the fact that for small α and ϵ its segment between the antidiagonal $a_1 = -a_2$ and the saddle is essentially straight, so we can find its intersection with the antidiagonal approximately by solving the system

$$\frac{a_2^s - a_2(0)}{a_1^s - a_1(0)} = \frac{a_2(0)\lambda_2}{a_1(0)\lambda_1}, \quad a_1(0) = -a_2(0), \quad (21)$$

which gives

$$a_2(0) = -a_1(0) = \frac{2(\beta + 1)}{3\beta} \sqrt{6} \sqrt{\alpha}. \quad (22)$$

Since according to Eq. (13) the optimal initial condition lies near, but not exactly on, the anti-diagonal $a_1 + a_2 = 0$, we should find the minimum of the norm (20) on the solution of the truncated model passing through Eq. (22), which coincides with the stable manifold. This can be done analytically since we can ignore the nonlinear terms in the first two equations in Eq. (15) near the antidiagonal. Solving the resulting system yields

$$a_1(t) = a_1(0)e^{\lambda_1 t} = O(\alpha^{1/2}),$$

$$a_2(t) = -a_1(0)e^{\lambda_2 t} = O(\alpha^{1/2}),$$

$$a_3(t) = O(\alpha^{5/2}) \qquad (23)$$

for $t = O(1)$. The norm of this solution is given by

$$\|A\mathbf{a}\|_2 = |a_1(0)| \sqrt{\left|\frac{9}{4}\epsilon e^{\lambda_1 t}\right|^2 + |U(t)|^2 + \left|\frac{9}{8}\epsilon e^{\lambda_1 t}\right|^2}, \quad (24)$$

where, to leading order in α, the term

$$U(t) = e^{\lambda_2 t} - \left(\frac{\epsilon}{2} + 1\right)e^{\lambda_1 t} \approx \frac{\epsilon}{2}(4t - 1)\alpha \qquad (25)$$

vanishes at $t = 1/4$. Substituting this value into Eq. (24) we obtain the norm of the critical optimal initial disturbance leading to destabilization

$$\sigma_2 = \frac{9}{8}\sqrt{\frac{5L}{2}}|a_1(0)|\epsilon e^{(1/4)\lambda_1} = \frac{9\sqrt{10\pi}}{8}(\beta + 1)\alpha^{3/2} \quad (26)$$

to leading order in α.

　　To verify these results we use the full system described by the PDE (1) to compute numerically the critical noise level σ_2. The results are shown in Fig. 3 along with the prediction (26) of the three mode truncation. Again one finds quantitative agreement for a wide range of β, despite the approximations made in computing the stable manifold.

　　From Eq. (26) it is clear that in the present model we do not get a simple scaling relationship between the magnitude of critical disturbances σ_2 and the transient amplification factor Γ. For instance, if we choose β to be constant (including $\beta = 0$), $\Gamma \propto \alpha^{-1}$ which yields $\sigma_2 \propto \alpha^{3/2} \propto \Gamma^{-3/2}$. However, in the opposite limiting case $\beta \to \infty$ (or $\epsilon \gg \alpha$) we have $\Gamma \propto \epsilon^{-1}$, so that $\sigma_2 \propto \epsilon\sqrt{\alpha}$ does not scale as a power law of Γ, unless α scales as some power of ϵ. In either case destabilization of the uniform state occurs for smaller magnitudes of disturbances compared with the "linear" scenario characterized by the scaling exponent $\kappa = -1$, i.e., $\sigma_2 \propto \Gamma^{-1}$.

　　This lower value of the exponent would have indeed been obtained in our model, if it were not for the emergence of saddles near the origin. In their absence destabilization of the uniform state would have corresponded to trajectories crossing the edges of the band $|a_1 + a_2| < s^*$. The critical disturbances touching the edge of the band would have had $|\mathbf{a}(0)| = O(s^*) = O(1)$, so that $\sigma_2 \propto \Gamma^{-1}$ for arbitrary α and ϵ. However, since the stable manifolds of the saddles lie completely inside the band, this scenario is never realized.

V. TRANSIENT DYNAMICS WITH A QUADRATIC NONLINEARITY

　　Next we turn to the quadratic nonlinearity, $f(\phi) = \phi^2$, which arguably has more significance due to its connection with shear fluid flows. In this case, Eq. (6) yields
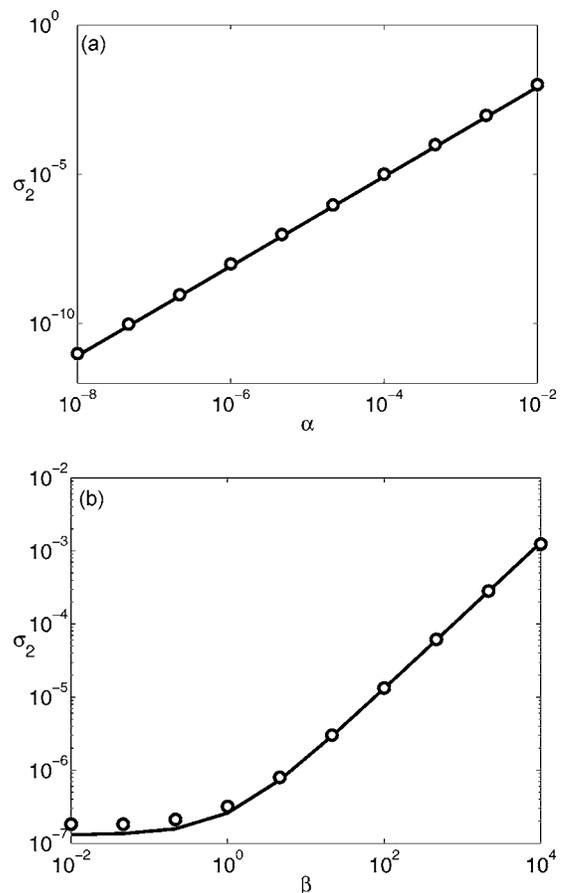
FIG. 3. Critical noise level σ_2 (a) as function of α with $\beta = 1$ and (b) as a function of β with $\alpha = 10^{-5}$. The circles show the numerical results for the PDE (1) and the solid line represents the analytical result (26).

$$\dot{a}_1 = \lambda_1' a_1 - \frac{32s^2}{35\pi\epsilon},$$

$$\dot{a}_2 = \lambda_2' a_2 + \frac{32s^2}{35\pi\epsilon},$$

$$\dot{a}_3 = \lambda_3' a_3 + \frac{180s^2}{77\pi} + \frac{680sa_3}{819\pi} + \frac{764a_3^2}{495\pi}. \qquad (27)$$

As in the previous section, adiabatic elimination of a_3 requires finding the fixed points of the last equation in Eq. (27). There are two, $a_3^{\pm} = u \pm v$, where

$$v = \frac{10}{17381}\sqrt{1002001\pi^2 - 935935\pi s - 4356992s^2},$$

$$u = \frac{110}{191}\pi - \frac{4675}{17381}s. \qquad (28)$$

One can find a_3^- to be stable and a_3^+ unstable for $s_-^* < s < s_+^*$, where
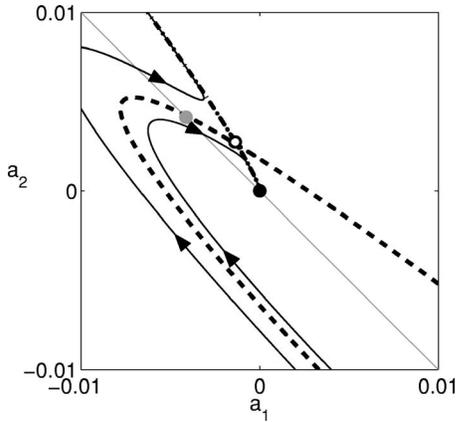
FIG. 4. The phase portrait of the system with the quadratic nonlinearity for $\alpha = 10^{-2}$ and $\beta = 1$. Closed and open black circles denote, respectively, the nodes and saddles of the truncation (27). The dashed and dash-dotted lines show, respectively, the stable and unstable manifolds of the saddles. The solid black curves show sample trajectories of the PDE (1). The gray circle represents the estimate (32) of the intersection between the stable manifold and the antidiagonal $a_1 = -a_2$ (solid gray line).

$$s_-^* = -\frac{117117\sqrt{1337} + 935935}{8713984}\pi \approx -1.88,$$

$$s_+^* = \frac{117117\sqrt{1337} - 935935}{8713984}\pi \approx 1.21. \quad (29)$$

At $s = s_\pm^*$ the two fixed points collide and disappear in a saddle node bifurcation. Consequently any initial condition leading to a trajectory crossing the, now asymmetric, band $s_-^* < |a_1 + a_2| < s_+^*$ leads to the blow up of a_3 and immediate destabilization of the uniform state $\phi = 0$, just as for the cubic nonlinearity.

However, in this case again the dominant destabilization mechanism is different. As long as the trajectory stays inside the band, we can replace a_3 in the first two equations in Eq. (27) with the stable fixed point value

$$a_3^- = \frac{405}{308\pi}s^2 + \frac{34425}{56056\pi}s^3 + \cdots. \quad (30)$$

Substituting this expansion into Eq. (27) we find that the system possesses a stable node at the origin and a saddle

$$a_1^s = -\frac{35\pi}{16}\frac{(1+\beta)}{\beta}\alpha^2,$$

$$a_2^s = \frac{35\pi}{16}\frac{(1+\beta)^2}{\beta}\alpha^2. \quad (31)$$

The critical disturbance in this case again corresponds to a trajectory that evolves along the separatrix defined by the stable manifold of the saddle fixed point (see Fig. 4).

Again, instead of computing the stable manifold exactly, we will exploit the fact that for small α and ϵ its segment between the antidiagonal $a_1 = -a_2$ and the saddle is essentially straight, so we can find its intersection with the antidi-
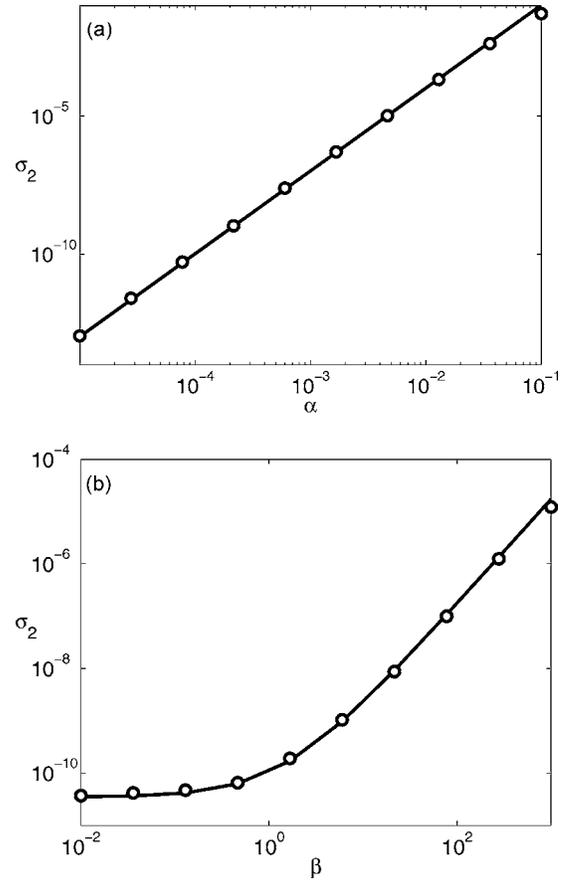

FIG. 5. Critical noise level σ_2 (a) as function of α with $\beta = 1$ and (b) as a function of β with $\alpha = 10^{-4}$. The circles show the numerical results for the PDE (1) and the solid line represents the analytical result (33).

agonal approximately by solving the system (21) which gives

$$a_2(0) = -a_1(0) = \frac{35\pi}{16}\frac{(1+\beta)(2+\beta)}{\beta}\alpha^2. \quad (32)$$

The norm of the critical optimal initial disturbance leading to destabilization is obtained in the same way as in the previous case. Specifically, we find

$$\sigma_2 = \frac{9}{8}\sqrt{\frac{5L}{2}}|a_1(0)|\epsilon e^{(1/4)\lambda_1} = \frac{21(15\pi)^{3/2}}{256}(1+\beta)(2+\beta)\alpha^3, \quad (33)$$

to leading order in α.

To verify this result we compute numerically the critical noise level σ_2 for the PDE (1). The results are shown in Fig. 5 along with our analytical result. Again we find quantitative agreement between our three mode truncation (27) and the full system for a wide range of β.

Here too we do not get a simple scaling relationship between σ_2 and Γ. For instance, if we choose β to be constant (zero or nonzero), then $\Gamma \propto \alpha^{-1}$ which yields $\sigma_2 \propto \alpha^3 \propto \Gamma^{-3}$.

However, for $\beta \rightarrow \infty$ we have $\sigma_2 \propto \epsilon^2 \alpha$ which again does not scale as a power law of $\Gamma \propto \epsilon^{-1}$ unless α scales as some power of ϵ.

VI. SUMMARY AND CONCLUSIONS

To summarize, we have constructed a spatially extended model with pronounced transient dynamics which allows analytic description of nonlinear stability. The study of this model allowed us to connect quantitatively the transient behavior with the effect of nonlinearities in describing the "bypass" transitions. Specifically, we have found that destabilization of the uniform state in our model can follow two qualitatively different routes.

In the simplest scenario, the destabilization mechanism is essentially linear. No steady states emerge in the vicinity of the uniform state and while the strongly stable degrees of freedom remain frozen out, the weakly stable degrees of freedom display pronounced transient dynamics well described by a generalized linearized stability analysis. It is the destabilization of the slaved strongly stable directions that leads to transition. In the context of control, the situation is similar to the "control spillover" effect described by Mezic *et al.* [19], where stabilization of the previously unstable degrees of freedom leads to destabilization of the previously stable degrees of freedom at large magnitudes of noise. The critical magnitude of noise in this case is found to scale inversely proportional to the transient amplification factor, i.e., with exponent $\kappa = -1$ while the basin of attraction of the uniform state forms a cropped band in the space of strongly non-normal weakly stable modes.

For the two types of nonlinearities considered here, however, we find that a different destabilization mechanism dominates. This second mechanism is intrinsically nonlinear in the sense that nonlinear terms play a crucial role in the dynamics of both weakly stable (transient) and strongly stable (slaved) degrees of freedom. The key players in this second scenario are unstable (saddle) steady states that emerge in the vicinity of the linearly stable uniform state. It is the stable manifolds of these saddles that form the boundary of the basin of attraction of the uniform state.

We found that the spatial structure of the smallest magnitude disturbances that can cause destabilization of the uniform state (i.e., nonlinearly optimal disturbances) is close, but not identical, to the spatial structure of the infinitesimal disturbances that achieve the largest transient growth (i.e., linear optimal disturbances). The critical magnitude of nonlinearly optimal disturbances is determined by the smallest norm of all initial conditions lying on the stable manifold of one of the saddle points in the vicinity of the uniform state and to leading order their magnitude is given by the intersection of the stable manifold by the line defining linear optimal disturbances.

Specifically, we find that the exponents describing the scaling of critical disturbances are nonuniversal: for $L \approx \frac{3}{2}\pi$ the critical noise level scales as a power of transient amplification factor Γ with exponent $\kappa = -3/2$ (cubic nonlinearity) or $\kappa = -3$ (quadratic nonlinearity) only when the transient time scale ϵ^{-1} and the time scale of asymptotic exponential decay α^{-1} scale in the same way with system parameters (such as the Reynolds number R in case of shear flows). If the two time scales were not directly proportional, the value of the exponent would change or an altogether different scaling behavior would be found. We also find that for small L the exponents differ from those for large L ($\kappa = -1$ for the cubic) and ($\kappa = -2$ for the quadratic nonlinearity).

Interestingly, typical shear flows do fall in the class of systems for which a power law scaling is expected: for both plane Couette and pipe Poiseuille flow one finds $\alpha \propto \epsilon \propto R^{-1}$ so that our simple model would predict $\sigma \propto \alpha^3 \propto R^{-3}$ for a quadratic nonlinearity. This is exactly the generic scaling predicted by a number of phenomenological low-dimensional models of transition [10]. However, both the asymptotic analysis of the plane Couette flow [11] and the experiments performed for the pipe Poiseuille flow [8] find power law scaling $\sigma \propto R^{-1}$ with exponent rather different from the one predicted by these low-dimensional models as well as our model.

The saddles we found are direct analogs of saddle type solutions found in shear fluid flows [5,20–22], but while the role of such solutions is only speculated in the context of transition in shear fluid flows, our model unambiguously shows that their stable and unstable manifold indeed organize the dynamics in the vicinity of the uniform state. In particular, our model explains why such unstable solutions can be experimentally observable. They provide the bottlenecks through which the system can escape from the origin near onset of instability, so in an appropriately tuned experiment (such as the pipe flow experiment described in Ref. [23]) the fluid flow will spend a considerable amount of time in the vicinity of one of such saddles before either returning to the uniform state or escaping towards a turbulent state along the corresponding unstable manifold.

Some studies [24] suggest that turbulence is described by a chaotic repellor with the flow state transiently visiting a multitude of such saddle states before eventually returning (in the absence of noise) to the laminar state. If so, one should expect to see successive secondary instabilities reflecting the dynamics of the system evolving along the stable and unstable manifolds of different saddles. To see similar phenomena in a simplified model such as the one considered here at least a pair of saddles unrelated by symmetry is needed. Our model, however, is only weakly nonlinear and so only describes the dynamics near the saddles closest to the origin. One could in principle modify the nonlinear terms to introduce, and study, the dynamics involving more saddles using our basic approach.

[1] J. Kim and R. D. Moser, Phys. Fluids A **1**, 775 (1989).

[2] L. N. Trefethen, A. E. Trefethen, S. C. Reddy, and T. A. Driscoll, Science **261**, 578 (1993).

[3] S. Grossmann, Rev. Mod. Phys. **72**, 603 (2000).

[4] E. Reshotko, Phys. Fluids **13**, 1067 (2001).

[5] F. Waleffe, Phys. Fluids **15**, 1517 (2003).

[6] B. F. Farrell and P. J. Ioannou, J. Atmos. Sci. **53**, 2025 (1996).

[7] B. Bamieh and M. Dahleh, Phys. Fluids **13**, 3258 (2001).

[8] B. Hof, A. Juel, and T. Mullin, Phys. Rev. Lett. **91**, 244502 (2003).

[9] E. B. White, Phys. Fluids **14**, 4429 (2002).

[10] J. Baggett and L. Trefethen, Phys. Fluids **9**, 1043 (1997).

[11] S. J. Chapman, J. Fluid Mech. **451**, 35 (2002).

[12] R. O. Grigoriev and A. Handel, Phys. Rev. E **66**, 067201 (2002).

[13] R. O. Grigoriev and A. Handel, Phys. Rev. E **66**, 065301(R) (2002).

[14] A. Handel and R. O. Grigoriev, Phys. Rev. E **72**, 066208 (2005).

[15] F. Waleffe, Phys. Fluids **9**, 883 (1997).

[16] J. Moehlis, H. Faisst, and B. Eckhardt, New J. Phys. **6**, 56 (2004).

[17] R. A. Horn and C. R. Johnson, *Matrix Analysis* (Cambridge University Press, Cambridge, 1985).

[18] G. H. Golub and C. F. van Loan, *Matrix Computations* (The John Hopkins University Press, Baltimore, 1996).

[19] G. Hagen and I. Mezić, Proceedings of the 2000 American Control Conference (American Auto. Control Council, Danvers, MA, 2000), Vol. 6, p. 3783.

[20] O. Dauchot and N. Vioujard, Eur. Phys. J. B **14**, 377 (2000).

[21] T. Itano and S. Toh, J. Phys. Soc. Jpn. **70**, 703 (2001).

[22] J. D. Skufca, J. A. Yorke, and B. Eckhardt, Phys. Rev. Lett. **96**, 174101 (2006).

[23] B. Hof, C. W. H. van Doorne, J. Westerweel, H. F. F. T. M. Nieuwstadt, B. Eckhardt, H. Wedin, R. R. Kerswell, and F. Waleffe, Science **305**, 1594 (2004).

[24] H. Faisst and B. Eckhardt, J. Fluid Mech. **504**, 343 (2004).